GEOPHYSICAL RESEARCH LETTERS, VOL. 35, L17103, doi:10.1029/2008GL034987, 2008

Angular beaming model of Jupiter's decametric radio emissions based on Cassini RPWS data analysis

Masafumi Imai,[1] Kazumasa Imai,[2] Charles A. Higgins,[3] and James R. Thieman[4]

Received 11 June 2008; revised 16 July 2008; accepted 7 August 2008; published 13 September 2008.

[1] Observations of the low frequency part of Jupiter decameter wavelength (DAM) emissions were made using the Cassini radio and plasma wave science (RPWS) instrument. We have analyzed non-Io-DAM occurrence dependence from 4 MHz to 16 MHz based on the System III central meridian longitude (CML) of the Cassini spacecraft and calculated the occurrence probability for each frequency. As a result of this analysis, the two peaks of non-Io-B and non-Io-A occurrence probability showed a dramatic change in longitude between 9 MHz and 16 MHz. At 16 MHz two peaks of probability occurred at 160° and 240° CML. As the frequency decreases to 9 MHz, the two peaks converged to become one peak near 205° CML at 9 MHz. This peak gradually disappeared below 9 MHz. Based on Jupiter's magnetic VIP4 model, an angular beaming model was made to explain these observational results by taking into account the decreasing cone half-angle of the emitting cone from 16 MHz down to 9 MHz. We found the active magnetic flux tubes of non-Io-B and non-Io-A sources are localized at about 180° ± 10° of System III longitude projected on Jupiter's surface. **Citation:** Imai, M., K. Imai, C. A. Higgins, and J. R. Thieman (2008), Angular beaming model of Jupiter's decametric radio emissions based on Cassini RPWS data analysis, *Geophys. Res. Lett.*, *35*, L17103, doi:10.1029/2008GL034987.

1. Introduction

[2] It is well known that Jupiter's decametric radiation is strongly affected by Jupiter's magnetic System III longitude and the orbital position of the satellite Io [*Bigg*, 1964]. This influence can be clearly seen on the map of Jupiter's radio occurrence probability plotted as a function of the central meridian longitude (CML) of System III (1965) and the departure angle of the satellite Io from superior geocentric conjunction (Io phase). The frequency range of Jupiter's DAM radio emission is considered to be from a few megahertz to nearly 40 MHz. As the observable lower frequency at ground stations is limited by terrestrial ionospheric conditions, only the higher frequency part above about 15 MHz can be observed from earth. At about 20 MHz there are three significant well-known zones where occurrence probabilities are relatively high. They are called sources B, A, and C, in increasing longitude sequence [*Carr et al.*, 1983]. It is known that the emission is almost elliptically or circularly polarized, in the right-hand sense for sources A and B, and often in the left-hand sense for source C. The emission is believed to be radiated in the R-X mode at a frequency just above the local electron gyrofrequency [*Carr et al.*, 1983]. Therefore sources A and B are considered to be located in the northern auroral zone and the source C in the southern auroral zone. Each source consists of Io-controlled and non-Io-controlled components, the former being observed only within a relatively narrow range of Io phase.

[3] The Io-controlled components (Io-DAM) are believed to originate along Jovian magnetic field lines with the shell parameter L-shell $\approx$ 5.9 (i.e., a dipolar magnetic field line from the planet's center intersects the equatorial plane at a distance of 5.9 planetary radii), belonging to the previously energized flux tube which has a relatively large lead angle downstream of Io [*Imai et al.*, 1997]. Meanwhile, the L-shell value of the sources of the non-Io controlled DAM (non-Io-DAM) has been thought to extend along L-shell $\geq$ 7 field lines [see *Zarka*, 1998; *Clarke et al.*, 2004, and references therein]. But measurement by the modulation lane method shows the source L-shell value is close to 5.9 inside the Io plasma torus region [*Imai et al.*, 2002].

[4] The purpose of this paper is to report the result of a statistical study of the low frequency part of non-Io-DAM radio emission from 4 MHz to 16 MHz by using Cassini data, providing new information not only on the beam structure of the radiation, but also on the location of its source.

2. Data and Observations

[5] The Cassini spacecraft was equipped with the radio and plasma wave science (RPWS) instrument having five on-board receivers that monitored the electric fields from 1 Hz to 16 MHz. The high frequency receiver (HFR) covers the frequency range from 3.5 kHz to 16 MHz and consists of two sets of four analog receivers with a digital signal processing unit. It is connected to three 10 m long monopole electric field antennas, called here E_U, E_V, and E_W. These are used to receive electric field signals. The E_U and E_V monopoles were configured at an angle of 120° and both nearly orthogonal to the E_W monopole. For a full description of the RPWS instrument see *Gurnett et al.* [2004]. For the present study, only the upper band of HFR (HF2) was used. Our analyzed mode of HF2 had a sweep period of 32 seconds for all frequency channels from 4.025 MHz to 16.025 MHz, each channel having a 200 kHz bandwidth.

[1]Advanced Course in Mechanical and Electrical Engineering, Kochi National College of Technology, Kochi, Japan.
[2]Department of Electrical Engineering, Kochi National College of Technology, Kochi, Japan.
[3]Department of Physics and Astronomy, Middle Tennessee State University, Murfreesboro, Tennessee, USA.
[4]Solar System Exploration Division Services Office, NASA Goddard Space Flight Center, Greenbelt, Maryland, USA.

0094-8276/08/2008GL034987$05.00

[6] The closest approach to Jupiter of the Cassini spacecraft on its way to Saturn occurred 30 December 2000. We have analyzed DAM emissions from 2 October 2000 to 21 March 2001 by using HF2 data observed with E_U, E_V, and E_W monopoles, respectively. The range of the spacecraft Jovicentric latitude is from +3.7° (2 October 2000) to −3.7° (21 March 2001). There is an equivalent of 281 Jupiter rotation periods (1 rotation = 9 hours 55 minutes) of data used in this study. All of the Jovian CML and Io phase values were sampled extensively.

3. Analysis and Modeling

[7] The Cassini data from 4 MHz to 16 MHz are calibrated and normalized to the intensity of 100 R_J distance for each frequency channel. The data are compiled for spacecraft flyby and organized by Jupiter's rotation. The data are sorted into 5° bins of Jovian CML and 5° bins of Io phase. All bins were observed at least 44 times. Moreover, 97% of the bins were observed above 120 times.

[8] For each rotation of Jupiter, a detection threshold was calculated for each frequency channel as the mean intensity (μ) plus one fifth the standard deviation (σ) of the mean ($\mu + 0.2\sigma$) at E_U, E_V, and E_W monopoles, respectively. This "rotation-based" averaging for the threshold allows for better analysis by removing any local time effects and long term changes in data reception. If we increase the threshold (larger than 0.2σ), the number of samples gets too small to perform statistical analysis. Also, if we lower the threshold too much, then we introduce all the low intensity emissions. We are interested in intensities a significant amount larger than the mean intensities for each rotation. Adding minimally low intensity emissions will reduce the occurrence probability effect.

[9] The compiled data are best displayed as probability of occurrence graphs sorted by Jovian CML and Io phase. This relative occurrence probability is a calculated value between 0 and 1 for each longitude and Io phase bin as the total number of activity counts above the rotation threshold intensity divided by the total number of observation counts for each bin [*Higgins et al.*, 2006; *Higgins*, 2007]. An activity count occurs when the radio emission intensity is above the rotation-based threshold for that particular frequency at that particular CML and Io phase value. An observation count occurs when the receiver is operating nominally for that particular time period. The total occurrence probability was calculated by the combination of the received data from the three individual monopole antennas. Concerning the antenna directivity pattern of the single monopole antenna, the axis direction is considered to be null point. This method avoids the null effect of any single monopole antenna for statistical analysis.

[10] The results of the analysis at 16.025 MHz are shown in Figure 1a plotted as a function of Jovian CML and Io phase. The enhancements in occurrence probability are seen for the Io phase near 90° and 250°. This is consistent with the previous study of Jupiter's low frequency radiation from 2 MHz to 14 MHz [*Alexander et al.*, 1981; *Kaiser and Garcia*, 1997; *Aubier et al.*, 2000]. Although there are distinct Io-DAM emissions in Figure 1a, non-Io-DAM components can be clearly seen. Especially, non-Io-B appears more prominent than ground based observations.

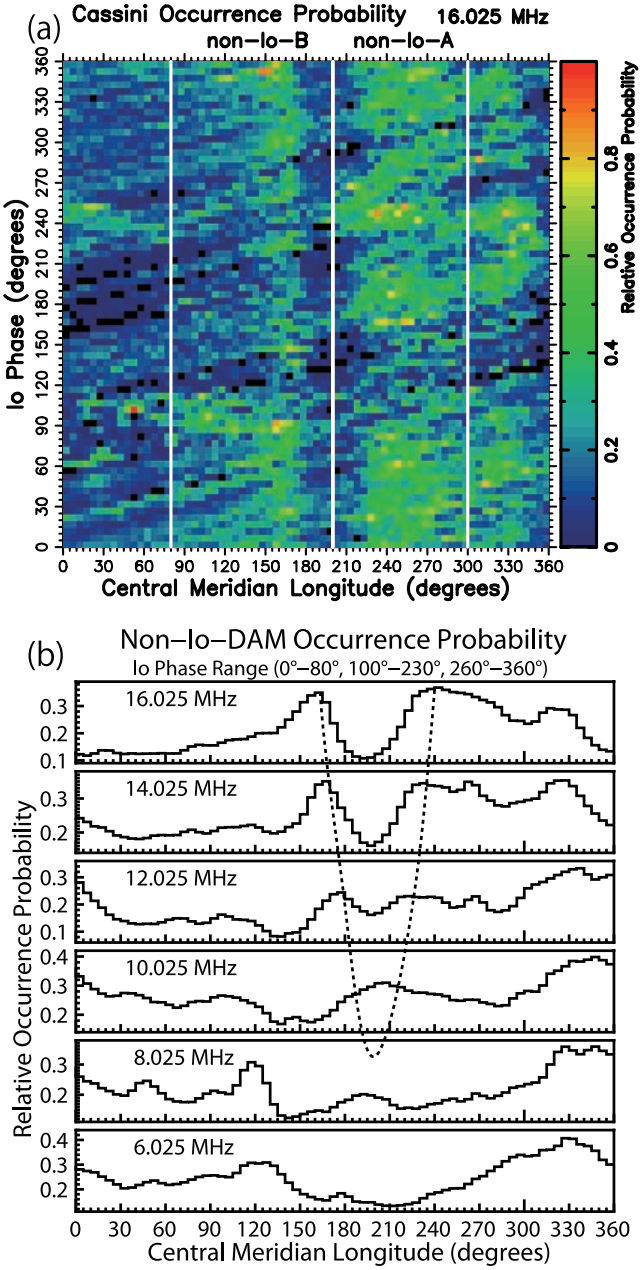

Figure 1. (a) Cassini data at 16.025 MHz are shown as a probability of occurrence graph of Jovian CML versus Io phase. The occurrence probability color scale is shown at the right. The area between 80° and 200° CML indicates the non-Io-B region, and the area between 200° and 300° indicates non-Io-A [cf. *Carr et al.*, 1983]. (b) This graph is a histogram of relative occurrence probability as a function of Jovian CML from 6.025 MHz to 16.025 MHz in 2 MHz steps.

To investigate the dependency of the System III longitude for radio sources of the non-Io-B and non-Io-A, we removed the data having an Io phase between 85° and 100° and between 235° and 260°, for each frequency [*Higgins et al.*, 2006; *Higgins*, 2007].

[11] Figure 1b shows Jovian CML versus relative occurrence probability from 16.025 MHz down to 6.025 MHz

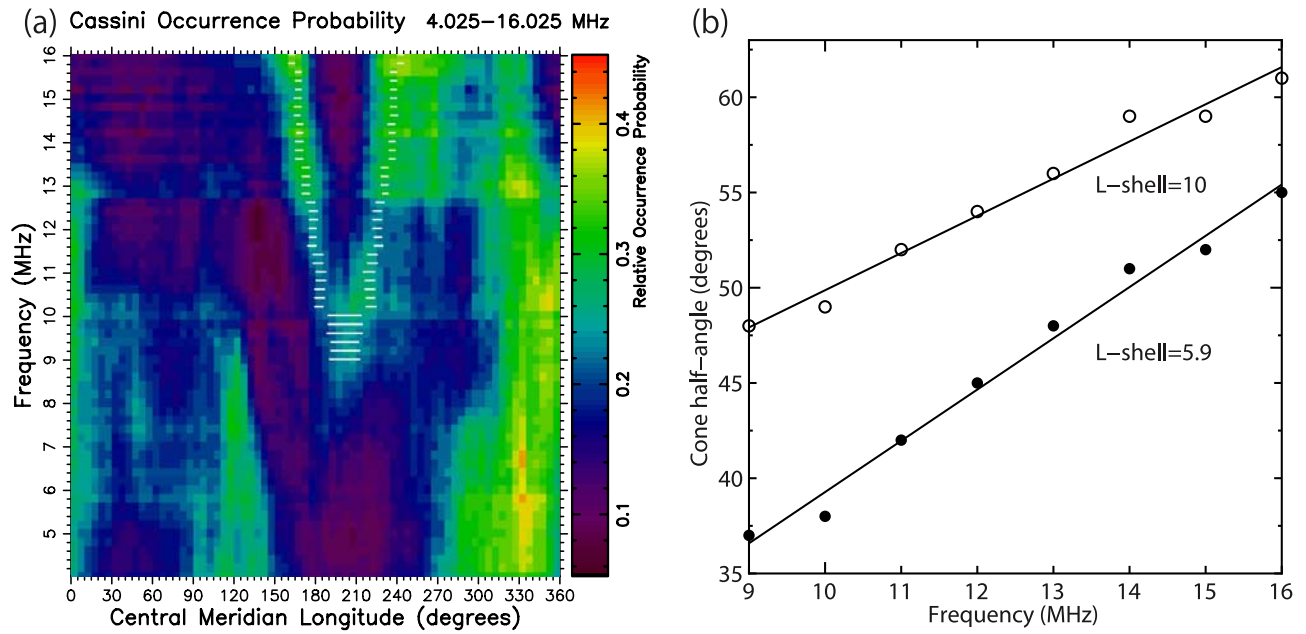

Figure 2. (a) Occurrence probability of non-Io-DAM from 4 MHz to 16 MHz is shown as a function of Jovian System III CML. The white horizontal lines represent the best fit of the 198° active magnetic flux tube at L-shell = 5.9. (b) This graph plots the best fitting cone half-angle of the V-shape pattern versus frequency from 9 MHz to 16 MHz for 1 MHz intervals at L-shell = 5.9 and 10.

every 2 MHz. The two peaks of non-Io-B and non-Io-A in occurrence probability showed a dramatic change in longitude between 6.025 MHz and 16.025 MHz. At 16.025 MHz two peaks of probability occurred at 160° and 240° CML. As the frequency decreases to 10.025 MHz, the two peaks converged to become one peak near 205° at 10.025 MHz. This peak gradually disappeared below 10.025 MHz in Figure 1b. Although we have to take into account the local time effects [*Alexander et al.*, 1981] and beaming effects [*Carr et al.*, 1983], the morphology of the pattern looks very much like a V-shape, which is shown by the dotted line in Figure 1b.

[12] To see the fine structure of the V-shape we calculated the occurrence probability from 4.025 MHz to 16.025 MHz in 200 kHz steps (61 channels) as a function of Jovian CML in Figure 2a. We also corrected the relative occurrence probability for a few of the frequency channels to reduce nearly continuous interference generated by the spacecraft itself. Figure 2a shows the frequency of the lower point of the V-shape is close to 9 MHz. The enhancement of the occurrence probability above 300° CML from 4 MHz to 16 MHz is considered to be the combination of hectometer wavelength (HOM) emissions and non-Io-C emissions. Also, the emissions between 90° to 145° CML below 9 MHz are considered to be another part of HOM emissions. The analysis of these HOM emissions will be the subject of a future paper.

[13] We now discuss the V-shape pattern of non-Io-B and non-Io-A in Figure 2a. During early study of Jupiter's radio emissions by ground based observation, *Thieman and Smith* [1978] found a substantial drift in the source A and B peaks from 10 MHz to 15 MHz based on analyzing the 19 years of data from 5.6 MHz to 30 MHz at the Universities of Florida and Texas. *Alexander et al.* [1981] found the peaks of sources A and B are drifting in CML to merge as they both broaden in the Voyager 2 post encounter measurements of average flux density from 22 MHz down to 12 MHz. However, *Thieman and Smith* [1978] and *Alexander et al.* [1981] did not exclude the effect of Io in their analyses. Recently, *Kaiser and Garcia* [1997] and *Aubier et al.* [2000] made an occurrence probability map based on combined data sets with frequency from 2 MHz to 14 MHz by using Wind/WAVES in 1995 and 1996, but they could not find the characteristics of the V-shape pattern because of the integration effects toward frequency direction and the low sensitivity of the receiving system.

[14] In modeling the observed V-shape pattern, we assumed that the radio sources are located along the active magnetic flux tubes and straight-line propagation of radio emissions [*Ladreiter and Leblanc*, 1990, and references therein] from a source region at frequencies approximately equal to the local electron cyclotron frequencies. In calculating the source locations and wave normal angles we have used the VIP4 magnetic field model [*Connerney et al.*, 1998]. In this model we hold the position of the observer (Cassini) at a fixed radial distance r = $100R_J$ and at latitude = 0°. As the L-shell values of the active magnetic flux tubes of non-Io-DAM can be free parameters, we selected two L-shell values, 5.9 and 10. The former is based on the results of *Imai et al.* [2002]. The latter is chosen to check the dependence on the larger L-shell values. And the beam structure is considered to be a fixed thin hollow cone beam which has less than 2° thickness [*Kaiser et al.*, 2000].

[15] Figure 2a shows the observable range of the superposition on the occurrence probability graph as white horizontal lines estimating the cone half-angle at the 198° active magnetic flux tube (the projected System III longitude on Jupiter's surface is 181°) at L-shell = 5.9 by our model. The width of the white lines shows the observable

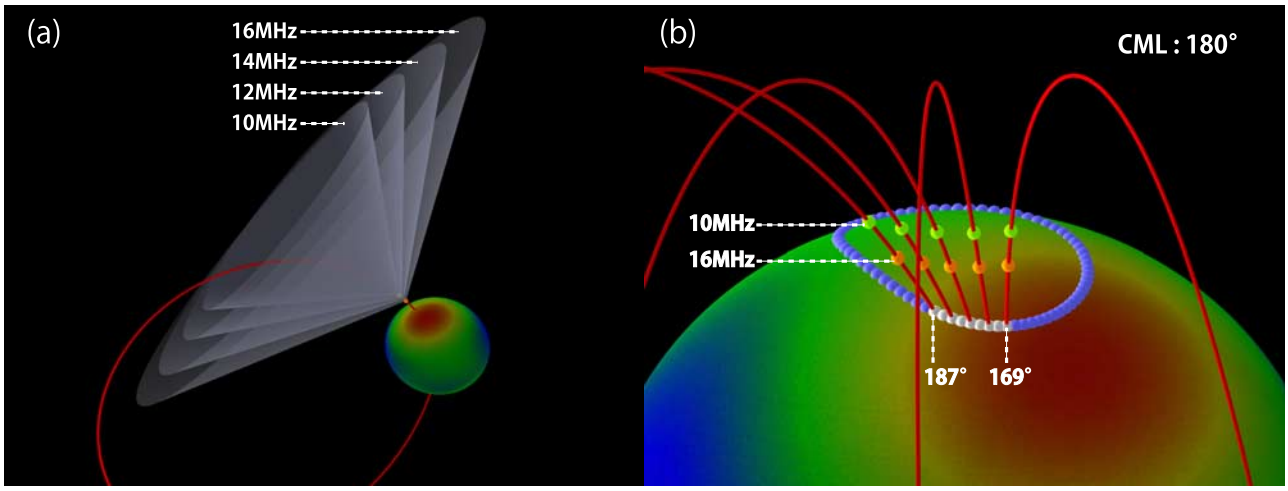

Figure 3. 3D computer graphic (CG) images of the geometry of the emitting cones and the source locations based on VIP4 model in the case of L-shell = 5.9. Color coded contour shows the magnitude of the magnetic field on the surface of Jupiter. (a) The emitting cones having the variation of the cone half-angle from 10 MHz to 16 MHz every 2 MHz at the 198° active magnetic flux tube. (b) The locations of the feet of the active magnetic flux tubes (169°–187°) are indicated by the small white dots along the otherwise blue contour line. The red lines indicate the active magnetic flux tubes intersecting Io's orbit from 170° to 210° CML every 10°. The source locations of the green and the orange spheres correspond to the electron gyrofrequency at 10 MHz and 16 MHz, respectively.

range at the cone half-angle of the emitting cone ±1°. The emitting cone with 55° cone half-angle at 16 MHz intersects two sections in relation to the observer, at 162° ± 2° and 242° ± 2° in System III CML in Figure 2a. As the frequency decreases to 9 MHz, the emitting cone with 37° cone half-angle crossed only one section, between 190° and 212° in System III CML. In Figure 2b we show the calculated cone half-angle versus frequency plots, from 9 MHz to 16 MHz in 1 MHz steps to fit the V-shape pattern for L-shell values 5.9 and 10.

[16] In the case of L-shell = 10, the change of the value of the cone half-angle is slightly different, but the trend of the decreasing cone half-angle from 16 MHz down to 9 MHz is similar to the L-shell = 5.9 case. We have also investigated the source locations by using the peak width of the non-Io-B source between 140° and 170° CML at 16.025 MHz in Figure 1b. At L-shell = 5.9 the corresponding range of System III longitude of the intersection of the active magnetic flux tubes with the equatorial plane is from 170° to 210° (the range of the projected longitude on Jupiter's surface is from 169° to 187°). By contrast, at L-shell = 10 the range is from 165° to 210° (the projected range is from 167° to 185°). It means both non-Io-B and non-Io-A sources are localized at about 180° ± 10° of System III longitude projected on Jupiter's surface. Figure 3a shows the emitting cones with the decreasing cone half-angle for frequencies from 10 MHz to 16 MHz in 2 MHz steps by using 3D computer graphics. And also, Figure 3b shows the active magnetic flux tubes of non-Io-B and non-Io-A sources.

4. Summary and Conclusions

[17] In this paper we report non-Io-B and non-Io-A occurrence dependence on CML. When occurrence probability for CML is plotted versus emitting frequency, it looks very much like a V-shape pattern (see Figure 2a). We have proposed a changing angular beaming model to explain this pattern by taking into account the decreasing cone half-angle of the emitting cone from 16 MHz down to 9 MHz. By using our model we found the active magnetic flux tubes of non-Io-B and non-Io-A sources are localized at about 180° ± 10° of System III longitude projected on Jupiter's surface.

[18] It is widely believed that non-Io-DAM is auroral radio emission from the Jovian aurora. *Prangé et al.* [1993] state that one of the characteristics of an intense auroral event in December 1990 was a shift in longitude from the statistical average value of near 180° to greater longitudes by about 60°. Recently, the complex structures of the Jovian UV aurora have been obtained by the Hubble Space Telescope [*Clarke et al.*, 2004]. *Waite et al.* [2001] found the strong intensity flare appeared near 167° System III longitude. During the Cassini campaign, a polar flare also occurred on 14 December 2000 around 170° System III longitude [*Grodent et al.*, 2003]. Our results of 180° ± 10° are close to the values of longitudes of these UV aurora phenomena. The close relationship between UV aurora and non-Io-DAM emission can be considered.

[19] The electron cyclotron maser instability (CMI) is considered to be the mechanism responsible for Jupiter's decametric radiation [*Wu and Lee*, 1979]. The angular dependence of the growth rate is very sensitive to the ratios ω_{pe}^2/Ω_e^2 and n_e/n_b [*Wong et al.*, 1982; *Wu*, 1985], where ω_{pe}^2 and Ω_e^2 are the electron plasma frequency and the electron cyclotron frequency, and n_e and n_b are the number densities of the energetic and background electrons. *Wong et al.* [1982] and *Wu* [1985] showed the growth rates vary with wave normal angle. Although we do not yet fully understand the plasma parameters around the radio emitting region, future theoretical study might explain why the emission cone half-angles have this dependence on frequency. We believe that the emitting cone half-angle dependence on

frequency is the key parameter of the local plasma environment of the emitting source region.

[20] **Acknowledgments.** The authors are pleased to acknowledge the Cassini RPWS team for access to Cassini data at the Planetary Data System (PDS) and J. Groene for creating Cassini ephemeris tables. The authors are especially grateful to A. Lecacheux and H. Misawa for numerous discussions. This work was supported by the Ministry of Education, Culture, Sports, Science and Technology, Grant-in-Aid for Scientific Research (B), 19340142.

References

Alexander, J. K., T. D. Carr, J. R. Thieman, J. J. Schauble, and A. C. Riddle (1981), Synoptic observations of Jupiter's radio emissions: Average statistical properties observed by Voyager, *J. Geophys. Res.*, *86*, 8529–8545.

Aubier, A., M. Y. Boudjada, P. Moreau, P. H. M. Galopeau, A. Lecacheux, and H. O. Rucker (2000), Statistical studies of Jovian decameter emissions observed during the same period by Nancay Decameter Array (France) and WAVES experiment aboard Wind spacecraft, *Astron. Astrophys.*, *354*, 1101–1109.

Bigg, E. K. (1964), Influence of the satellite Io on Jupiter's decametric emission, *Nature*, *203*, 1008–1010.

Carr, T. D., M. D. Desch, and J. K. Alexander (1983), Phenomenology of magnetospheric radio emissions, in *Physics of the Jovian Magnetosphere*, edited by A. J. Dessler, pp. 226–284, Cambridge Univ. Press, New York.

Clarke, J. T., D. Grodent, S. W. H. Cowley, E. J. Bunce, P. Zarka, J. E. P. Connerney, and T. Satoh (2004), Jupiter's aurora, in *Jupiter: The Planet, Satellites and Magnetosphere*, edited by F. Bagenal, T. E. Dowling, and W. B. McKinnon, pp. 639–670, Cambridge Univ. Press, New York.

Connerney, J. E. P., M. H. Acuña, N. F. Ness, and T. Satoh (1998), New models of Jupiter's magnetic field constrained by the Io flux tube footprint, *J. Geophys. Res.*, *103*, 11,929–11,939.

Grodent, D., J. T. Clarke, J. H. Waite Jr., S. W. H. Cowley, J.-C. Gérard, and J. Kim (2003), Jupiter's polar auroral emissions, *J. Geophys. Res.*, *108*(A10), 1366, doi:10.1029/2003JA010017.

Gurnett, D. A., et al. (2004), The Cassini radio and plasma wave investigation, *Space Sci. Rev.*, *114*, 395–463.

Higgins, C. A. (2007), Satellite control of Jovian 2–6 MHz radio emission using Voyager data, *J. Geophys. Res.*, *112*, A05213, doi:10.1029/2006JA012100.

Higgins, C. A., J. D. Menietti, and I. W. Christopher (2006), Europa control of Jovian radio emission: A Galileo study, *Geophys. Res. Lett.*, *33*, L14110, doi:10.1029/2006GL026218.

Imai, K., L. Wang, and T. D. Carr (1997), Modeling Jupiter's decametric modulation lanes, *J. Geophys. Res.*, *102*, 7127–7136.

Imai, K., J. J. Riihimaa, F. Reyes, and T. D. Carr (2002), Measurement of Jupiter's decametric radio source parameters by the modulation lane method, *J. Geophys. Res.*, *107*(A6), 1081, doi:10.1029/2001JA007555.

Kaiser, M. L., and L. N. Garcia (1997), Jupiter's low-frequency radio spectrum: Filling in the gaps, in *Planetary Radio Emissions IV*, edited by H. O. Rucker, S. J. Bauer, and A. Lecacheux, pp. 17–24, Austrian Acad. Sci., Vienna.

Kaiser, M. L., P. Zarka, W. S. Kurth, G. B. Hospodarsky, and D. A. Gurnett (2000), Cassini and Wind stereoscopic observations of Jovian nonthermal radio emissions: Measurement of beam widths, *J. Geophys. Res.*, *105*, 16,053–16,062.

Ladreiter, H. P., and Y. Leblanc (1990), Source location of the Jovian hectometric radiation via ray-tracing technique, *J. Geophys. Res.*, *95*, 6423–6435.

Prangé, R., P. Zarka, G. E. Ballester, T. A. Livengood, L. Denis, T. Carr, F. Reyes, S. J. Bame, and H. W. Moos (1993), Correlated variations of UV and radio emissions during an outstanding Jovian auroral event, *J. Geophys. Res.*, *98*, 18,779–18,791.

Thieman, J. R., and A. G. Smith (1978), Frequency and time dependence of the Jovian decametric radio emissions: A nineteen-year high-resolution study, *J. Geophys. Res.*, *83*, 3303–3309.

Waite, J. H., Jr., et al. (2001), An auroral flare at Jupiter, *Nature*, *410*, 787–789.

Wong, H. K., C. S. Wu, F. J. Ke, R. S. Schneider, and L. F. Ziebell (1982), Electromagnetic cyclotron-loss-cone instability associated with weakly relativistic electrons, *J. Plasma Phys.*, *28*, 503–525.

Wu, C. S. (1985), Kinetic cyclotron and synchrotron maser instabilities: Radio emission processes by direct amplification of radiation, *Space Sci. Rev.*, *41*, 215–298.

Wu, C. S., and L. C. Lee (1979), A theory of the terrestrial kilometric radiation, *Astrophys. J.*, *230*, 621–626.

Zarka, P. (1998), Auroral radio emissions at the outer planets: Observations and theories, *J. Geophys. Res.*, *103*, 20,159–20,194.

C. A. Higgins, Department of Physics and Astronomy, Middle Tennessee State University, Murfreesboro, TN 37132, USA. (chiggins@mtsu.edu)

K. Imai, Department of Electrical Engineering, Kochi National College of Technology, Monobe, Nankoku, Kochi, Japan 783-8508. (imai@ee.kochi-ct.ac.jp)

M. Imai, Advanced Course in Mechanical and Electrical Engineering, Kochi National College of Technology, Monobe, Nankoku, Kochi, Japan 783-8508. (masafumi@jupiter.jp)

J. R. Thieman, Solar System Exploration Division Services Office, NASA Goddard Space Flight Center, Code 690.1, Greenbelt, MD 20771, USA. (james.r.thieman@nasa.gov)